Mitochondrial plasticity in the cerebellum of two anoxia-tolerant sharks: Contrasting responses to anoxia/reoxygenation.

Jules B.L. Devaux[1], Anthony J.R. Hickey[1], Gillian M.C Renshaw[2].

[1] School of Biological Sciences, The University of Auckland, Auckland 1142, New Zealand.

[2] Hypoxia and Ischemia Research Unit, School of Allied Sciences, Griffith University, Gold Coast campus, QLD 4222, Australia.

Corresponding author:

Jules Devaux
School of Biological Sciences
The University of Auckland
Private Bag 92019
Auckland Mail Centre
Auckland 1142
New Zealand
Email: devauxjules@gmail.com
+64 (21) 1422411

Keywords: Mitochondria, anoxia-tolerance, succinate, brain, shark, oxygen

Summary statement: The brain mitochondria of reef sharks reveals some adaptations that parallels their contrasted physiological strategies to cope against environmental oxygen deprivation.

Abstract

Exposure to anoxia leads to rapid ATP depletion, alters metabolic pathways and exacerbates succinate accumulation. Upon re-oxygenation, the preferential oxidation of accumulated succinate most often impairs mitochondrial function. Few species can survive prolonged periods of hypoxia and anoxia at tropical temperatures and those that do may rely on mitochondria plasticity in response to disruptions to oxygen availability. Two carpet sharks, the epaulette shark (*Hemiscyllium ocellatum*; ES) and the grey carpet shark (*Chiloscyllium punctatum*; GCS) display different adaptive responses to prolonged anoxia: while the ES enters energy conserving metabolic depression, the GCS temporarily elevates its haematocrit prolonging oxygen delivery. High-resolution respirometry was used to investigate mitochondrial function in the cerebellum, a highly metabolically active organ that is oxygen sensitive and vulnerable to injury after anoxia/re-oxygenation (AR).

Succinate was titrated into cerebellar preparations *in vitro*, with or without pre-exposure to AR, then the activity of mitochondrial complexes was examined. Like most vertebrates, GCS mitochondria significantly increased succinate oxidation rates, with impaired complex I function post-AR. In contrast, ES mitochondria inhibited succinate oxidation rates and both complex I and II capacities were conserved, resulting in preservation of oxidative phosphorylation capacity post-AR.

Divergent mitochondrial plasticity elicited by elevated succinate post A/R parallels the inherently divergent physiological adaptations of these animals to prolonged anoxia, namely the absence (GCS) and presence of metabolic depression (ES). Since anoxia tolerance in these species also occurs at temperatures close to that of humans, examining their mitochondrial responses to AR could provide insights for novel interventions in clinical settings.

Introduction

An adequate and continuous supply of oxygen is fundamental to fuelling vertebrate respiration. If the supply of oxygen is severely diminished in mammalian species, survival is limited to a few minutes unless they have adaptations to survive deep sea diving, hibernation or stress-induced torpor. In the absence of specialised biochemical and physiological readjustments, hypoxia or anoxia can compromise cellular energy supplies, triggering signal cascades that result in organ failure and subsequently death. Sub-cellularly, anoxia can result in irreversible damage to mitochondria (Andrienko et al., 2017; Javadov, 2015) which can induce the release cytochrome *c*, an initiator of cell death by apoptosis (Kinnally et al., 2011). Furthermore, majority of cell damage occurs during the re-introduction of normal oxygen levels (Kalogeris et al., 2012). Mitochondrial dysfunction does not always lead to cell death, for example, diminished mitochondrial transmembrane potential can be re-established by 72 hours post-stress (Tuan et al., 2008).

In species that evolved their anoxia tolerance at temperatures close to 0°C, the duration of extreme anoxia-tolerance can extend to months, because hypothermia slows enzymatic reactions, diffusion and energy consuming processes, all of which spare energetic resources (Rubinsky, 2003). However, the increase in energy consumption associated with increased metabolic rates in species adapted to higher temperatures (~20-25°C), diminishes the survival time for anoxia-tolerant species to a few days or even hours (Lutz and Nilsson, 1997). On tropical reef platforms temperatures of up to 35ºC have been observed (Potts and Swart,

1984) and remarkably some are inhabited by hypoxia and anoxia-tolerant reef sharks that have evolved their survival mechanisms in the absence of cold-induced survival mechanisms (Nilsson and Renshaw, 2004). Only a few fish have evolved survival mechanisms that protect them from hypoxia and anoxia in tropical environments, such as: African lakes (Chapman et al., 2002), the Amazon (Richards et al., 2007; Val et al., 2015; Val, 1998), and warm coral reef waters (Nilsson and Ostlund-Nilsson, 2004; Renshaw et al., 2002; Routley et al., 2002). Since some of these tropical hypoxia and anoxia-tolerant species can survive several hours of hypoxia at mammalian temperatures in contrast to the a few minutes that humans are able to tolerate, they make useful experimental models in which to examine protective mechanisms.

The epaulette shark (*Hemiscyllium ocellatum*) and its close relative the grey carpet shark (*Chiloscyllium punctatum*) represent ancestral vertebrates and are the only elasmobranch species reported to tolerate prolonged anoxia or hypoxia at tropical temperatures (Chapman and Renshaw, 2009; Wise et al., 1998). The grey carpet shark (CGS) is distributed in northern Australian waters and is widely distributed in Indo-West Pacific regions (Dudgeon, 2016) while the epaulette shark (ES) is restricted to northern Australian waters and New Guinea (Bennett, 2015; Chapman and Renshaw, 2009; Last, 2009). Both species have been observed on reef flats during the day. While the ES has been observed hunting and feeding on reef flats during nocturnal hypoxic conditions, it has not been confirmed whether the GCS occupy this niche on nocturnal low tides. However, under experimental conditions the GCS can sustain around 1h anoxia at 25°C, while the ES routinely survives 2.5h (Chapman et al., 2011; Renshaw et al., 2002; Routley et al., 2002). The ES is capable of metabolic depression and neuronal hypometabolism in response to diminished oxygen (Mulvey and Renshaw, 2000; Stenslokken et al., 2008) through mediators such as adenosine receptors (Renshaw et al., 2002). Neuronal hypometabolism and temporary blindness may act to diminish the demand for ATP (Mulvey and Renshaw, 2000; Stenslokken et al., 2008). The ES increased the production of NO in response to hypoxia, which could enhance oxygen delivery (as discussed in Nilsson and Renshaw, 2004; Renshaw and Dyson, 1999) and depresses mitochondrial O_2 consumption (Brown, 1995; Cooper and Brown, 2008). In addition, ES are naturally exposed to cycles of nocturnal hypoxia in their natural environment (Nilsson and Renshaw, 2004), which has been demonstrated pre-condition this species for longer future exposures to hypoxia with early entry into ventilatory and metabolic depression (Routley et al., 2002).

In contrast, the GCS maintain their metabolic and ventilation rates, and rapidly increased their haematocrit in response to anoxia, most likely *via* splenic contractions (Chapman and Renshaw, 2009). It was suggested that the O_2 from stored red blood cells could be released which would ultimately increase the supply of oxygen to metabolically active organs when the O_2 supply is compromised.

It has been proposed that oxidative damage originates during re-oxygenation from an increase in mitochondria derived reactive oxygen species ("ROS"; illustrated in **Fig. 6**), potentially triggering apoptosis and necrosis (Murphy, 2009). While laboratory-based anoxic stress can be well tolerated by both shark species (Chapman and Renshaw, 2009), there is evidence of re-oxygenation induced oxidative damage in the ES (Renshaw et al., 2012) even though the ES produced less reactive species than other elasmobranchs (Hickey et al., 2012). In mammals, it has been demonstrated that succinate accumulates in highly metabolic ischemic organs (at least in the brain, heart, liver and kidney) as a result of the ischemia induced reversal of the succinate dehydrogenase (SDH i.e. mitochondrial complex II or CII) and the partial inhibition of the malate/aspartate shuttle (Chouchani et al., 2014). Upon reperfusion, succinate is oxidised at elevated rates and this drives excess ROS production by

the reversal of electron flow at complex I (CI) (discussed in Andrienko et al., 2017). This succinate-induced ROS can cause oxidative damage that alters mitochondrial function (Paradies et al., 2002) (illustrated in **Fig. 6**). These detrimental effects of reperfusion in the presence of excess succinate may be further enhanced at elevated temperatures (De Groot and Rauen, 2007).

Intriguingly, the anoxia-tolerant ES displayed greater mitochondria membrane stability after an anoxic event than the hypoxia-sensitive shovelnose ray (*Aptychotrema rostrata*) (Hickey et al., 2012). It was proposed that the high mitochondrial membrane stability observed in the ES would act to maintain oxidative phosphorylation (*Oxphos*) efficiency and decrease ROS production post-anoxia, which would decrease oxidative damage mediated by re-oxygenation (Hickey et al., 2012). Although ES heart mitochondria are robust in response to an anoxic challenge, the effect of succinate build-up and ROS production on mitochondria respiratory complexes and mitochondrial efficiency in other highly metabolic tissues such as the brain, have yet to be determined. The cerebellum is one of the most vulnerable regions of the brain to damage from a hypoxic insult (Cervós-Navarro and Diemer, 1991). The loss of the righting reflex, controlled by the cerebellum, is the first sign of physiological shut down and evidence suggests that such cerebellar shut down acts to conserve brain energy charge (Renshaw et al., 2002). In addition, the ES cerebellum: (i) increases the transcription of pro-survival genes in response to recurrent hypoxic preconditioning (Rytkonen et al., 2012); and (ii) makes protective proteomic readjustments following episodes of either hypoxic or anoxic preconditioning (Dowd et al., 2010). It should be noted that cytochrome oxidase levels are significantly decreased by exposure to diminished oxygen, representing neuronal hypometabolism (Mulvey and Renshaw, 2000), which implies that mitochondria turn down ETS activity in response to hypoxia. This questions whether cerebellum mitochondria are plastic in their response to diminished oxygen and whether they can subsequently recover

To test whether mitochondrial plasticity is likely to be involved in the tolerance of the ES and/or the GCS brain to anoxia, we investigated the tolerance of mitochondria in whole preparations from the cerebellum of each species to an acute episode of anoxia/re-oxygenation (AR) with and without elevated succinate levels. More specifically, we compared the mitochondrial respiratory capacity and the mitochondrial plasticity (readjustment of respiratory pathway from CI and CII) in responses to graded levels of exogenous succinate in mitochondria exposed to either AR or maintained with sufficient O_2 (controls). Using high resolution respirometry, we tested the hypothesis that the cerebellum mitochondria from ES cerebellum would be more resilient to AR compared to those from the GCS and that ES mitochondria would adjust their respiratory characteristics in response to graded exogenous succinate rather than exhibit high CII succinate oxidation rates during reoxygenation. This is the first report describing both i) the normal activity of ES and GCS intact mitochondrial population in the cerebellum; and ii) their responses to an anoxic challenge followed by re-oxygenation. Both experiments were carried out with graded exogenous succinate.

Materials and methods

1.1. Animals and housing

Six sub-adult ES with a mean of 490 ± 83 g were purchased from Cairns Marine (Cairns, Australia) while seven sub-adult GCS with a mean of 138 ± 31 g were provided by Sea World (Main Beach, Gold Coast, Australia). Sharks were held in 300L tanks containing

aerated sea water maintained at 22°C and fed daily with fresh raw shrimps. After a week of acclimation, sharks were starved for two days prior to euthanasia and the commencement of high-performance mitochondrial respirometry. The sharks were measured and weighed post-euthanasia and the cerebellum was weighed prior to homogenisation.

1.2. Cerebellum preparation

Tissue homogenates which avoided shear stress, were chosen over other methods of preparation (i.e. permeabilised brain or isolated mitochondria) because they retain i) mitochondrial integrity; ii) all sub-populations of mitochondrial *in situ*; and iii) conserve potential cellular regulators of mitochondrial function (Kondrashova et al., 2009). However, while including the overall mitochondrial characteristics of different sub-populations contained in the shark cerebellum, any potential differences in mitochondrial density were not assessed. Consequently, the reported difference in respiration rates between the two sharks provide information on the overall mitochondrial capacity within a fixed mass of shark cerebellum, and is not intended to examine differences between mitochondrial units (i.e. adjustments within a mitochondrion).

Sharks were euthanized by the addition of 15 ml of 5% benzocaine, dissolved in ethanol, to 1L sea-water for a final dose of 750 mg benzocaine/L. After ventilation ceased, the absence of response to fin pinch test and the loss of righting reflex indicated that euthanasia was complete, then the spinal cord was sectioned at the cranio-vertebral junction and sharks were rapidly dissected. The cerebellum was rapidly removed and immersed in ice-cold biopsy buffer (in mM: 2.77 CaK_2EGTA, 7.23 K_2EGTA, 5.77 Na_2ATP, 6.56 $MgCl_2.6H_2O$, 20 taurine, 15 Na_2Phosphocreatine, 20 imidazole, 0.5 DTT, 50 KMES, and 50 Sucrose, pH 7.1 at 30°C) (Hickey et al., 2012). Then the cerebellum was gently blotted, to remove excess blood and it was weighed into ~150 mg pieces in 800 µl cold MiR05 respiration medium (containing, in mM: 0.5 EGTA, 3 $MgCl_2.6H_2O$, 60 K-lactobionate, 20 taurine, 10 KH_2PO_4, 2.5 HEPES, 700 sucrose and 1g l^{-1} BSA essentially free fatty acid, pH 7.2 at 22°C). A portion of the diced cerebellum was gently homogenised by triturating the small pieces through a 10ml syringe with decreasing gauge needles (16-25 gauge) and allowed to recover for an hour in cold MiR05 prior to use in respirometry experiments.

1.3. Respirometry experiments

A multiple substrate uncoupler inhibitor protocol (SUIT) was performed to assess the effect of AR on: (i) The total proton leak (L_{Total}) and the inducible proton leak through adenine nucleotide translocase (L_{ANT}); (ii) complex I (CI) mediated respiration and O_2 flux (JO_2) attributed to *Oxphos* with and without succinate build-up; (iii) the electron transport system (ETS) capacity and (iv) CII capacity (**Fig. 1**). Electron inputs from either complex I or complex II can be assessed in SUIT protocols with the sequential reconstitution of TCA cycle pathways by the addition of complex specific substrates. The contribution of each complex to ETS reflects putative mitochondrial plasticity because it represents the readjustment of convergent electron pathways to *Oxphos* (detailled in Gnaiger, 2014). The addition of succinate and rotenone in the absence of CI substrate, mediates oxaloacetate accumulation and further competitively inhibits CII (Harris and Manger, 1969). In this study, the CII contribution to *Oxphos* was determined by the additive effect of excess succinate to CI-mediated *Oxphos* (with pyruvate, malate and glutamate) because additive electrons flow from CI to the Q-junction converges according to a $NADH^+$:succinate ratio of at least 4:1 (Gnaiger, 2014).

Whole homogenates from the cerebellum of either GCS or ES (100 µl corresponding to 10-15 mg tissue) were added to the 2 ml chambers of Oroboros O2ks™ respirometers containing aerated MiR05 media at 20°C (261.92 µM O_2 at 101.5 kPa barometric pressure). After signal stabilisation, 20 min recovery was sufficient to exhaust routine respiration, which remaining exhausted respiration was subtracted from the other mitochondrial states. Then, mitochondria CI-linked substrates, pyruvate and malate were added at saturated concentrations (10 and 5 mM respectively) to assess the non-phosphorylating state mediated by CI inputs (L_{CI}). Oxidative phosphorylation supported by pyruvate and malate (PM *Oxphos*) was then triggered by the addition of 700 µM ADP and the additional effect of glutamate on mitochondrial respiration was tested by the addition of 10 mM glutamate (CI-*Oxphos*). To test mitochondrial tolerance to anoxia-reoxygenation (AR), mitochondria were allowed to deplete the chamber O_2 then maintained in anoxia for 20 minutes following re-oxygenation (Hickey et al., 2012), the control group had fully aerated medium.

The amount of tissue in the homogenates (~10-15 mg) was chosen as this permitted anoxic levels to be reached within 30-50 min. After acute anoxic exposure, chambers were exposed to ambient air to re-oxygenate the media up to ~220 µM O_2 and recommence respiration. Once CI-*Oxphos* fluxes post-anoxia were determined, a succinate titration (0-10 mM) was started using an automated titration pump to mimic gradual succinate accumulation. To determine the contribution of AR to altered mitochondrial function, the control tissues were exposed to succinate titration alone in fully aerated medium. Oligomycin was added (Oli, 5 µM) to determine total *Leak* respiration from combined CI and CII inputs (L_{Total}). The fraction of proton leak through the adenine nucleotide translocase (L_{ANT}) was then determined as the difference between L_{Total} and the residual leak ($L_{Residual}$), measured by the addition of carboxy-atractyloside (cAtr, 5 µM) to inhibit the ANT. Respiration was then uncoupled from *Oxphos* using three injections of the protonopore carbonyl cyanide m-chlorophenyl hydrazone (CCCP, 0.5 µM each) to determine the ETS capacity (ETS_{max}). Then, CII capacity uncoupled from Oxphos ($CII_{uncoupled}$) was assessed by the addition of the CI inhibitor rotenone (0.5 µM), as this represents the maximum capacity of CII to fuel the ETS with electrons, without limitations of the phosphorylating system, and without competition for the Q-pool (Gnaiger, 2014). A representative trace of the SUIT protocol and its corresponding effects on mitochondrial respiration is presented in **Fig. 1**.

1.4. Data and statistical analysis

Respirometry fluxes were calculated in real-time with DatLab 6.0 software and expressed in pmol O_2 s^{-1} mg^{-1}. The data and calculations were transferred to Microsoft Excel (Office vs15.38). The complex I contribution to *Oxphos* was calculated as the difference between *CI-Oxphos* and L_{CI}. The CII respiration coupled to *Oxphos* ($CII_{coupled}$) was calculated as the difference between *Oxphos* and *CI-Oxphos*. The respiratory or acceptor control ratio (RCR) is a function of *Oxphos* coupling efficiency of a system (Gnaiger, 2014) and was calculated by the formula *Oxphos/Leak*. To estimate whereas damage to ETS may affect *Oxphos*, we calculated the net *Oxphos* control ratio (nOCR) as (*Oxphos* - Leak)/ETS. Dose response curves for succinate were fitted with the least-squares method using GraphPad Prism 7.0. In addition to the maximum respiration rate derived from the addition of succinate ($CII_{coupled}$) and the apparent Km ("aKm_S"; determined as the succinate concentration at which respiration was half of $CII_{coupled}$) the catalytic efficiency of CII ("CII_{cat}"; proxy for enzymatic efficiency, generally represented as V_{max} / Km), was also presented and calculated as CII_{coupl}/aKm_s.

It should be noted that the use of the term "mitochondria", expressed here, does not refer to normalised mitochondrial entities (i.e. if mitochondrial density were established) but denotes

the all of mitochondrial populations in situ within the cerebellar homogenates. Therefore, mitochondrial characteristics interpreted from respiration rates in the present study, yield information about the capacity of mitochondria in the overall tissue, which better indicate the responses that are likely occur in shark cerebellum *in vivo*. It cannot be assumed that all of the results are directly related to mitochondrial adjustments at the organelle level. The data that was used to calculate a number of ratios associated with mitochondrial complexes and leak states did not require quantification of mitochondrial density and the discussion of results is largely based on these ratios

The Shapiro-Wilk test was used to test for normal distributions. SPSS 23.0 or GraphPad Prism 7.0 were used to perform a *student t-test* when equality of variances was verified. Two-way ANOVA repeated measure and post-hoc with Turkey multiple comparison were performed to compare the effect of substrates-inhibitor on mitochondrial states, to compare the effect of AR on CI contribution and to compare the additive effect of succinate build-up on mitochondrial respiration rates across species. A significant difference was accepted at $p < 0.05$.

Results

1.5. Shark morphology

Sub-adult GCS and ES were used for this study. While the ES had a greater mean body mass than GCS (**Table 1**), the mean proportion of cerebella mass to body mass was greater in the GCS than in the ES. Neither length nor mass or sex affected mitochondrial function (factorial ANOVA, homogeneity of variance verified with Levene's test).

1.6. Interspecies comparison of cerebellar mitochondrial *respiration in fully aerated medium.*

While the stepwise addition of substrates or inhibitors influenced mitochondrial respiration ($F_{7,42} = 153$, $p < 0.001$; **Fig 2**) Turkey post-hoc tests revealed no significant differences in leak states (L_{Total} and L_{ANT}) or *Oxphos* states (CI-*Oxphos* and *Oxphos*) between these two closely related carpet shark species. However, ES homogenates had a significantly higher ETS capacity (ETS_{max}) per mass tissue than GCS mitochondria ($p < 0.001$). The ETS_{max} was ~20% and ~75% higher than *Oxphos* in the GSC and ES, respectively ($p < 0.003$).

1.7. Effect of anoxia/reoxygenation on mitochondria complexes in the two closely related carpet sharks.

The overall responses of *Oxphos* and ETS to AR as well as the contribution of CI and CII to *Oxphos* were analysed and compared for each species. While *Oxphos* was significantly decreased by AR in GCS homogenates ($p < 0.001$), *Oxphos* was maintained post AR in ES homogenates ($p = 0.15$; **Fig. 3**). In response to AR, the ETS_{max} was significantly decreased in both shark species with a decrease of ~31-34% ($p < 0.01$) relative to the pre-anoxic state (**Table 2**).

In mitochondria from GCS cerebella, there was a significant 31% decrease in CI respiration following AR with saturated CI substrates (**Fig. 3**), which was not compensated for by the 2.7-fold increase in the CII contribution to *Oxphos* ($p < 0.001$; **Fig. 3**). We note that this could account for the significant decrease of CI + CII *Oxphos* by 26% (corresponding to ~4 pmol O_2 s^{-1} mg^{-1}; $p = 0.04$; **Fig. 3**). Despite this loss in respiration, RCRs and nOCRs were

not affected by AR ($p > 0.6$, **Table 2**). In contrast, CI mediated respiration was unaffected by AR in mitochondria from ES cerebella (**Error! Reference source not found. & Fig. 3**) and while the level of *Oxphos* respiration was preserved (**Fig. 3**), RCRs were significantly decreased indicating an increase in uncoupled respiration in *Oxphos* ($p = 0.007$, **Error! Reference source not found.**). *Oxphos* capacity was also greater in the ES cerebella following AR with a conserved ~91% capacity compared to ~74% in GCS mitochondria ($p = 0.05$; % **Fig. 3**).

The contribution of CII to respiration was also tested in two settings (**Table 2**), coupled to *Oxphos* (i.e. actual contribution to *Oxphos*) and uncoupled to *Oxphos* (full CII capacity to contribute to ETS). In GCS homogenates not exposed to AR, $CII_{coupled}$ respiration was ~2 pmol O_2 s^{-1} mg^{-1} and accounted for only 21% of $CII_{uncoupled}$ ($p < 0.001$). While post AR the $CII_{coupled}$ increased by ~80% ($p = 0.03$) and matched $CII_{uncoupled}$, CII overall was diminished by 60% ($p < 0.001$). In contrast, $CII_{coupled}$ reached its full capacity in ES homogenates not exposed to AR and equated $CII_{uncoupled}$ (~3.5 pmol O_2 s^{-1} mg^{-1}). Post AR however, $CII_{coupled}$ flux was decreased by 35% and equated to 30% $CII_{uncoupled}$ only ($p = 0.02$).

1.8. Apparent proton leak.

In the normoxic control groups for ES and GCS, the L_{Total} was similar between species ($p = 0.65$; **Fig. 2** & **Fig. 4**). However, while AR did not affect L_{Total} in the GCS *mt*, it significantly increased L_{Total} by ~58% in ES mitochondria ($p = 0.02$; **Fig. 4**). There was no apparent difference in L_{ANT} between the control groups for two species during pre-AR respiration (**Fig. 4**). However, following AR the ES mitochondria showed a significant ~4-fold increase in L_{ANT} ($p = 0.035$) while L_{ANT} was unchanged in the mitochondria of GCS. Since the $L_{Residual}$ was similar in both species and not affected by AR ($p > 0.5$) the increase in L_{Total} in ES mitochondria reflected the increase in L_{ANT}.

1.9. Effects of titrated exogenous succinate on oxygen flux.

Both the succinate concentration and exposure to AR influenced CII mediated JO_2 ($F_{3.52}$, $p = 0.015$) (**Fig. 5**). In control groups, the apparent Km to succinate was similar between the two species (aKm_S ~0.4-0.9 mM). However, the $CII_{coupled}$ flux was two-fold higher in ES cerebella than in GCS cerebella ($p < 0.001$). In GCS, the CII fuelled respiration was significantly increased post-AR at succinate concentrations above 2 mM ($p < 0.05$). A Turkey post-hoc test revealed that the maximum CII-mediated respiration was significantly increased from 0.5 to 2.5 mM succinate in GCS ($p < 0.05$). Conversely in ES, AR mediated a significant decrease in CII fuelled respiration at succinate concentrations above 0.5 mM ($p < 0.01$), and the maximum CII mediated respiration was decreased at succinate concentrations above 2.5 mM (controls) or above 2 mM succinate in cerebellar preparations exposed to AR (**Fig. 5**). Exposure to AR increased the apparent Km to succinate in GCS mitochondria ($p < 0.001$) but not in ES mitochondria, in which aKm_S was unchanged (**Table 2**). While aKm_S was doubled in both species after exposure to AR, the capacity of CII to oxidise succinate CII_{cat} was maintained in GCS compared to their controls, while CII_{cat} was significantly decreased by ~35% relative to control groups in ES ($p < 0.001$; **Table 2**).

Discussion

Ultimately, surviving hypoxia or anoxia depends on an animal's ability to conserve energy stores by limiting their ATP demands and/or their ability to produce sufficient ATP despite O_2 limitations and the arrest of *Oxphos* (Boutilier, 2001). Notably, the ES had a smaller

cerebellum relative to their body mass than the GCS (**Table 1**). The metabolic scaling theory based on the relationship between body mass and metabolic rate (reviewed in Agutter and Wheatley, 2004) would support the notion that the cerebellum of ES may have lower demands for ATP and therefore require less O_2 to sustain cerebellar function than the cerebellum of GCS. In addition, the ES has the ability to undergo metabolic depression with clear evidence of neuronal hypometabolism (Mulvey and Renshaw, 2000; Stenslokken et al., 2008), which most likely enables the ES to withstand a longer exposure to limited environmental O_2. Although both species of carpet sharks are known to survive prolonged anoxia, the sharks displayed contrasting physiological responses in response to AR (Chapman and Renshaw, 2009). The *ex vivo* data collected in this study revealed that the contrasting mitochondrial plasticity of these two species of anoxia tolerant sharks parallels their *in vivo* physiological responses to anoxia: i) the mitochondria from the ES, capable of metabolic depression, decreased it metabolism of succinate in response to AR; while ii) the mitochondria from the GCS, which does not enter metabolic depression, not only continued to use succinate but also increased the rate of succinate metabolism in response to AR

1.10. Mitochondrial integrity with regard to anoxia/re-oxygenation

Cerebellum of the two carpet sharks displayed similar mitochondrial characteristics before exposure to AR *in vitro* (**Fig. 2**). While the data was not corrected for any differences in mitochondrial density, this finding implies that the cerebellum from both species had the same ability to produce ATP after AR. Both sharks had relatively high (reserve) ETS capacity (i.e. ETS > *Oxphos*), indicating that the cerebellum of both sharks can accommodate some damage to their ETS without a detrimental effect to *Oxphos* and ATP production rates. ETS damage may occur during reoxygenation because in the presence of O_2, electron leakage enhances ROS production and damage to lipids within biological membranes and this compromises ETS (Murphy, 2016; Musatov and Robinson, 2012; Paradies et al., 2002). We note that the ES cerebellum had a 20% greater ETS capacity than the GCS, which is likely to confer a substantial advantage against ROS damage in response to AR, due to the maintenance of high coupling and low leak state.

While AR decreased ETS by ~30% in both shark species, only the *Oxphos* rate in GCS cerebellum was affected with a 26% decrease. Previous work using permeabilised ES heart ventricle fibres, showed a ~20% to ~60% loss of ETS capacity relative to *Oxphos* following an anoxic exposure, with minimal change in *Oxphos* (Hickey et al., 2012) indicating a consistent response to anoxia in ES mitochondrial populations across cerebellum and heart tissues. Surprisingly, GCS homogenate respiration was more tightly coupled to *Oxphos* (greater RCR) than the ES homogenate. Furthermore, the net *Oxphos* ratio suggests similar ATP production efficiencies (i.e. similar nOCR) between the sharks. Overall, while *Oxphos* rates were lowered in both species, respiration in GCS was better coupled to *Oxphos* and hence more efficiently directed to ATP production. In contrast, respiration was less coupled to *Oxphos* in ES cerebellum but *Oxphos* rates were maintained post AR. Taken together, these data demonstrate that cerebella mitochondria exposed to AR appeared to experience ETS damage in both sharks, however ATP production rates may remain preserved with contrasting response between shark species.

1.11. Leak and contribution of the ANT

Proton leak results from protons dissipating passively or actively across the inner mitochondrial membrane without passing through the $ATP_{F0\text{-}F1}$ synthase, and therefore mediates a loss in coupling efficiencies of mitochondria (Divakaruni and Brand, 2011). The

total leak (L_{Total}, mediated with oligomycin) is similar for both species and represents around 10% of *Oxphos* rates, which corresponds to levels previously measures in ES heart mitochondria (Hickey et al., 2012). Although anoxia followed by reoxygenation did not affect total proton leak in the GCS cerebellum, AR significantly increased the total proton leak in ES cerebellum to 18% of *Oxphos* rates.

While counterintuitive, we note that increased proton leak can be beneficial, as it likely prevents elevated ROS production under reduced states (Ali et al., 2012; Rolfe and Brand, 1997), such as with elevated succinate with anoxia (Chouchani et al., 2014). Up to a third of total proton leakage occurs through the ANT (Azzu et al., 2008; Brand et al., 2005). The portion of L_{Total} attributed to the ANT increased from 43% pre-anoxia to 63% after AR in the ES. Similar increases have been observed in rodents displaying enhanced leak through the mitochondrial transition pore (and at least in part through the ANT) after repeated anoxia re-oxygenation episodes (Navet et al., 2006).

Proton leak through the ANT may reflect ADP-ATP exchange rates (Chinopoulos et al., 2014). This increase may therefore favour ADP-ATP exchange between mitochondria and the cytosol and restore cytosolic ATP and mitochondria ADP contents (Klingenberg, 2008). Overexpression of the ANT, *via* the activation of cell-protective pathways (ERK and AKT), has been shown to protect mammalian cardiomyocytes exposed to hypoxia (Winter et al., 2016) or oxidative stress (Klumpe et al., 2016). While the specific mechanisms of ANT regulation in ES mitochondria were not assessed in this study, elevated leak should decrease reverse electron flow, decrease localised O_2 concentration and therefore prevent increased ROS production (Brookes, 2005), and possibly temporarily increasing ATP-ADP exchange (**Fig. 6**).

1.12. Mitochondrial plasticity and complex contribution following AR

The capacity of CI and CII to feed the ETS with electrons is essential for the *Oxphos*. CI has been shown to be sensitive to anoxia (Chen et al., 2007; Giusti et al., 2008; Paradies et al., 2004; Rouslin, 1983) and the most sensitive mitochondrial complex to ROS damage (Hardy et al., 1990; McLennan and Degli Esposti, 2000; Paradies et al., 2004). In this study, CI contribution was tested prior to and after 20min anoxia. While the contribution of CI to *Oxphos* was similar for both species in normoxia, in the GCS mitochondria the CI capacity decreased by ~30% following AR (**Fig. 3**). The loss of CI JO_2 capacity was not fully compensated for by CII and resulted in an overall 26% loss in *Oxphos* capacity in the GCS mitochondria. However, the ES mitochondria which appeared to have a greater ETS reserve capacity also retained proportionately more CI supported flux following AR, despite a suppression in CII flux. Hence, O_2 utilisation in ES mitochondria is more efficiently transferred to proton pumping, essential for *Oxphos*.

In general, enhanced CII activity has been proposed to lead to a greater electron leakage from CII post-anoxia (Quinlan et al., 2012; Tretter et al., 2016; Zakharchenko et al., 2013), which may impact CI capacity through ROS-mediated oxidation of cardiolipin (Paradies et al., 2002). In hypoxia-tolerant drosophila, the suppression of CII activity decreased ROS production and was proposed to improve long-term survival in hypoxia (Ali et al., 2012). Hence, the data on CII suppression in ES following AR could have a role in preventing damage to CI upon reoxygenation (**Fig. 6**). In contrast, within the GCS cerebellum, CII was more sensitive to AR, yet provided a greater contribution to respiration than CI.

1.13. Succinate accumulation

In normoxic conditions, succinate is better utilised by the ES mitochondria with a greater CII contribution to *Oxphos* than GCS mitochondria (**Fig. 3**). Following anoxia, succinate is oxidised more rapidly by GCS mitochondria with increased apparent CII catalytic efficiencies. At high concentration (i.e above 2 mM), which approximate concentrations in ischemic mammalian brain (Benzi et al., 1979; Benzi et al., 1982; Folbergrova et al., 1974), succinate also mediated higher O_2 flux in GCS (**Fig. 4**). As enhanced succinate oxidation rates on reoxygenation can trigger reverse electron flow to CI, which impairs the mitochondrial function in murine model (Chouchani et al., 2014; Starkov, 2005), this may explain why CI capacities were decreased post-AR in the GCS.

In contrast, the overall mitochondrial succinate oxidation rates in the ES cerebellum were lowered in response to AR even with incremented succinate concentrations and this may suppress ROS production in the ES cerebellum (**Fig. 6**). Greater CII catalytic efficiency at low succinate concentrations also suggests that succinate is better utilised by ES cerebellum than by the GCS, which may prevent its accumulation. The downregulation of succinate dehydrogenase activity also occurs within ES rectal glands after hypoxic exposure (Dowd et al., 2010), and lowered succinate dehydrogenase has been shown to be protective against ischemia-reperfusion injuries in other animal models (Ali et al., 2012; Pfleger et al., 2015; Wojtovich and Brookes, 2008). Succinate oxidation is also depressed in hibernating squirrels, which experience reperfusion-like injury on arousal (Brown et al., 2012; Brown et al., 2013). While this is yet unknown whereas succinate accumulates in the cerebellum of the sharks, inhibition of succinate oxidation may reflect the metabolic suppression observed in the ES (Chapman et al., 2011; Renshaw and Dyson, 1999; Renshaw et al., 2002) furthermore it may account for the preconditioning effect initiated by a first anoxic exposure which remodelled responses to subsequent insults on a cellular level (Dowd et al., 2010; Rytkonen et al., 2012).

Conclusion

Contrasting responses of the GCS and the ES cerebella to AR with and without elevated succinate levels highlight key attributes of mitochondrial plasticity used by two tropical anoxia-tolerant species. Despite damage reflected by the decrease in ETS capacity post-AR in both species, *Oxphos* rates were not changed in the ES mitochondria and were only marginally lower in GCS mitochondria. In this respect, brain mitochondria in these two species are comparatively more robust than heart mitochondria from the anoxia sensitive shovelnose ray (Hickey et al., 2012).

GCS mitochondria were surprisingly more efficient in directing O_2 flux to *Oxphos* which could result in a greater capacity to produce ATP post-AR. A contrasting strategy which would maintain ATP levels post-AR was observed in ES mitochondria which had higher active proton leak rates associated with higher ADP/ATP exchange rates. Such a strategy would help to rapidly restore cytosolic energy stores post-AR.

The data revealed that CI was more robust to AR in ES cerebellum than in GCS cerebellum and that the partial inhibition of CII in the ES may represent the initiation of metabolic depression. Furthermore, CII inhibition in the ES would likely prevent reverse electron flow to CI. Such inhibition is likely to not only preserve CI integrity but also to limit ROS production during AR.

This study provides insights into the mitochondria physiology and plasticity in the brains of two anoxia tolerant tropical species which can tolerate hypoxia at temperatures close to that of the mammals. An understanding of how mitochondria plasticity occurs in tropical anoxia tolerant species could lead to novel therapeutic strategies to prevent ischemia-reperfusion injuries the mammalian brain.

Availability of Supporting Data
The data set supporting the result of this manuscript will be available at the University of Auckland repository upon manuscript acceptance.

List of Abbreviations:
aKm_S: Apparent Km for succinate

ANT: Adenine nucleotide translocase

AR: Anoxia/re-oxygenation

CCCP: carbonyl cyanide m-chlorophenyl hydrazone

CI: Mitochondrial complex I

CII: Mitochondrial complex II (or succinate dehydrogenase, SHD)

CII_{cat}: CII catalytic capacity

$CII_{coupled}$: CII capacity coupled to *Oxphos*

$CII_{uncoupled}$: CII capacity uncoupled from *Oxphos*

ES: Epaulette shark

ETS: Mitochondrial electron transport system

GCS: Grey carpet shark

JO_2: Mitochondrial respiration rate

L_{ANT}: Leak through adenine nucleotide translocase

$L_{Residual}$: Residual proton leak

L_{Total}: Total proton leak

Mt: Mitochondria

Oxphos: Oxidative phosphorylation

ROS: Reactive oxygen species

Competing interests
The authors declare no competing interests.

Acknowledgments

The authors would like to thank Dr. Oliva Holland, Dr Lan-feng Dong, and Professor Jiri Neuzil for graciously providing access to additional OROBOROS™ O2ks. We also thank Sea World (Gold Coast Australia) for supplying animals and the Smart Water Research Centre for their assistance with housing animals.

Funding

Epaulette sharks and chemicals were purchased personally by GMCR. JBLD, AJR and GMCR were supported by the Marsden funds of The Royal Society of New Zealand (14-UOA-210).

References

Agutter, P. S. and Wheatley, D. N. (2004). Metabolic scaling: consensus or controversy? *Theor Biol Med Model* **1**, 13.

Ali, S. S., Hsiao, M., Zhao, H. W., Dugan, L. L., Haddad, G. G. and Zhou, D. (2012). Hypoxia-adaptation involves mitochondrial metabolic depression and decreased ROS leakage. *PLoS One* **7**, e36801.

Andrienko, T. N., Pasdois, P., Pereira, G. C., Ovens, M. J. and Halestrap, A. P. (2017). The role of succinate and ROS in reperfusion injury - A critical appraisal. *J Mol Cell Cardiol* **110**, 1-14.

Azzu, V., Parker, N. and Brand, M. D. (2008). High membrane potential promotes alkenal-induced mitochondrial uncoupling and influences adenine nucleotide translocase conformation. *Biochem J* **413**, 323-32.

Bennett, M. B., Kyne, P.M. & Heupel, M.R. (2015). Hemiscyllium ocellatum. The IUCN Red List of Threatened Species 2015: e.T41818A68625284.

Benzi, G., Arrigoni, E., Marzatico, F. and Villa, R. F. (1979). Influence of some biological pyrimidines on the succinate cycle during and after cerebral ischemia. *Biochem Pharmacol* **28**, 2545-50.

Benzi, G., Pastoris, O. and Dossena, M. (1982). Relationships between gamma-aminobutyrate and succinate cycles during and after cerebral ischemia. *J Neurosci Res* **7**, 193-201.

Boutilier, R. G. (2001). Mechanisms of cell survival in hypoxia and hypothermia. *J Exp Biol* **204**, 3171-81.

Brand, M. D., Pakay, J. L., Ocloo, A., Kokoszka, J., Wallace, D. C., Brookes, P. S. and Cornwall, E. J. (2005). The basal proton conductance of mitochondria depends on adenine nucleotide translocase content. *Biochem J* **392**, 353-62.

Brookes, P. S. (2005). Mitochondrial H(+) leak and ROS generation: an odd couple. *Free Radic Biol Med* **38**, 12-23.

Brown, G. C. (1995). Nitric oxide regulates mitochondrial respiration and cell functions by inhibiting cytochrome oxidase. *FEBS Lett* **369**, 136-9.

Brown, J. C., Chung, D. J., Belgrave, K. R. and Staples, J. F. (2012). Mitochondrial metabolic suppression and reactive oxygen species production in liver and skeletal muscle of hibernating thirteen-lined ground squirrels. *Am J Physiol Regul Integr Comp Physiol* **302**, R15-28.

Brown, J. C., Chung, D. J., Cooper, A. N. and Staples, J. F. (2013). Regulation of succinate-fuelled mitochondrial respiration in liver and skeletal muscle of hibernating thirteen-lined ground squirrels. *J Exp Biol* **216**, 1736-43.

Cervós-Navarro, J. and Diemer, N. H. (1991). Selective vulnerability in brain hypoxia. *Critical reviews in neurobiology* **6**, 149-182.

Chapman, C. A., Harahush, B. K. and Renshaw, G. M. (2011). The physiological tolerance of the grey carpet shark (Chiloscyllium punctatum) and the epaulette shark (Hemiscyllium ocellatum) to anoxic exposure at three seasonal temperatures. *Fish Physiol Biochem* **37**, 387-99.

Chapman, C. A. and Renshaw, G. M. (2009). Hematological responses of the grey carpet shark (Chiloscyllium punctatum) and the epaulette shark (Hemiscyllium ocellatum) to anoxia and re-oxygenation. *J Exp Zool A Ecol Genet Physiol* **311**, 422-38.

Chen, Q., Camara, A. K., Stowe, D. F., Hoppel, C. L. and Lesnefsky, E. J. (2007). Modulation of electron transport protects cardiac mitochondria and decreases myocardial injury during ischemia and reperfusion. *Am J Physiol Cell Physiol* **292**, C137-47.

Chinopoulos, C., Kiss, G., Kawamata, H. and Starkov, A. A. (2014). Measurement of ADP-ATP exchange in relation to mitochondrial transmembrane potential and oxygen consumption. *Methods Enzymol* **542**, 333-48.

Chouchani, E. T., Pell, V. R., Gaude, E., Aksentijevic, D., Sundier, S. Y., Robb, E. L., Logan, A., Nadtochiy, S. M., Ord, E. N., Smith, A. C. et al. (2014). Ischaemic accumulation of succinate controls reperfusion injury through mitochondrial ROS. *Nature* **515**, 431-+.

Cooper, C. E. and Brown, G. C. (2008). The inhibition of mitochondrial cytochrome oxidase by the gases carbon monoxide, nitric oxide, hydrogen cyanide and hydrogen sulfide: chemical mechanism and physiological significance. *J Bioenerg Biomembr* **40**, 533-9.

De Groot, H. and Rauen, U. (2007). Ischemia-reperfusion injury: processes in pathogenetic networks: a review. *Transplant Proc* **39**, 481-4.

Divakaruni, A. S. and Brand, M. D. (2011). The regulation and physiology of mitochondrial proton leak. *Physiology (Bethesda)* **26**, 192-205.

Dowd, W. W., Renshaw, G. M., Cech, J. J., Jr. and Kultz, D. (2010). Compensatory proteome adjustments imply tissue-specific structural and metabolic reorganization following episodic hypoxia or anoxia in the epaulette shark (Hemiscyllium ocellatum). *Physiol Genomics* **42**, 93-114.

Dudgeon, C. L., Bennett, M.B. & Kyne, P.M. (2016). Chiloscyllium punctatum. The IUCN Red List of Threatened Species 2016: e.T41872A68616745.

Folbergrova, J., Ljunggren, B., Norberg, K. and Siesjo, B. K. (1974). Influence of complete ischemia on glycolytic metabolites, citric acid cycle intermediates, and associated amino acids in the rat cerebral cortex. *Brain Res* **80**, 265-79.

Giusti, S., Converso, D. P., Poderoso, J. J. and Fiszer de Plazas, S. (2008). Hypoxia induces complex I inhibition and ultrastructural damage by increasing mitochondrial nitric oxide in developing CNS. *Eur J Neurosci* **27**, 123-31.

Gnaiger, E. (2014). Mitochondrial Pathways and Respiratory Control: An Introduction to OXPHOS Analysis. *OROBOROS MiPNet Publications* **1**.

Hardy, D. L., Clark, J. B., Darley-Usmar, V. M. and Smith, D. R. (1990). Reoxygenation of the hypoxic myocardium causes a mitochondrial complex I defect. *Biochem Soc Trans* **18**, 549.

Harris, E. J. and Manger, J. R. (1969). Intersubstrate competitions and evidence for compartmentation in mitochondria. *Biochem J* **113**, 617-28.

Hickey, A. J., Renshaw, G. M., Speers-Roesch, B., Richards, J. G., Wang, Y., Farrell, A. P. and Brauner, C. J. (2012). A radical approach to beating hypoxia: depressed free radical release from heart fibres of the hypoxia-tolerant epaulette shark (Hemiscyllum ocellatum). *J Comp Physiol B* **182**, 91-100.

Javadov, S. (2015). The calcium-ROS-pH triangle and mitochondrial permeability transition: challenges to mimic cardiac ischemia-reperfusion. *Front Physiol* **6**, 83.

Kalogeris, T., Baines, C. P., Krenz, M. and Korthuis, R. J. (2012). Cell biology of ischemia/reperfusion injury. *Int Rev Cell Mol Biol* **298**, 229-317.

Kinnally, K. W., Peixoto, P. M., Ryu, S.-Y. and Dejean, L. M. (2011). Is mPTP the gatekeeper for necrosis, apoptosis, or both? *Biochim Biophys Acta* **1813**, 616-622.

Klingenberg, M. (2008). The ADP and ATP transport in mitochondria and its carrier. *Biochim Biophys Acta* **1778**, 1978-2021.

Klumpe, I., Savvatis, K., Westermann, D., Tschope, C., Rauch, U., Landmesser, U., Schultheiss, H. P. and Dorner, A. (2016). Transgenic overexpression of adenine nucleotide translocase 1 protects ischemic hearts against oxidative stress. *J Mol Med (Berl)* **94**, 645-53.

Kondrashova, M., Zakharchenko, M. and Khunderyakova, N. (2009). Preservation of the in vivo state of mitochondrial network for ex vivo physiological study of mitochondria. *Int J Biochem Cell Biol* **41**, 2036-50.

Last, P. R. (2009). Sharks and rays of Australia. Collingwood, Vic.: Collingwood, Vic. CSIRO Publishing 2009.

Lutz, P. L. and Nilsson, G. E. (1997). Contrasting strategies for anoxic brain survival--glycolysis up or down. *J Exp Biol* **200**, 411-9.

McLennan, H. R. and Degli Esposti, M. (2000). The contribution of mitochondrial respiratory complexes to the production of reactive oxygen species. *J Bioenerg Biomembr* **32**, 153-62.

Mulvey, J. M. and Renshaw, G. M. (2000). Neuronal oxidative hypometabolism in the brainstem of the epaulette shark (Hemiscyllium ocellatum) in response to hypoxic pre-conditioning. *Neurosci Lett* **290**, 1-4.

Murphy, M. P. (2009). How mitochondria produce reactive oxygen species. *Biochem J* **417**, 1-13.

Murphy, M. P. (2016). Understanding and preventing mitochondrial oxidative damage. *Biochem Soc Trans* **44**, 1219-1226.

Musatov, A. and Robinson, N. C. (2012). Susceptibility of mitochondrial electron-transport complexes to oxidative damage. Focus on cytochrome c oxidase. *Free Radic Res* **46**, 1313-26.

Navet, R., Mouithys-Mickalad, A., Douette, P., Sluse-Goffart, C. M., Jarmuszkiewicz, W. and Sluse, F. E. (2006). Proton leak induced by reactive oxygen species produced during in vitro anoxia/reoxygenation in rat skeletal muscle mitochondria. *J Bioenerg Biomembr* **38**, 23-32.

Nilsson, G. E. and Ostlund-Nilsson, S. (2004). Hypoxia in paradise: widespread hypoxia tolerance in coral reef fishes. *Proc Biol Sci* **271 Suppl 3**, S30-3.

Nilsson, G. E. and Renshaw, G. M. (2004). Hypoxic survival strategies in two fishes: extreme anoxia tolerance in the North European crucian carp and natural hypoxic preconditioning in a coral-reef shark. *J Exp Biol* **207**, 3131-9.

Paradies, G., Petrosillo, G., Pistolese, M., Di Venosa, N., Federici, A. and Ruggiero, F. M. (2004). Decrease in mitochondrial complex I activity in ischemic/reperfused rat heart: involvement of reactive oxygen species and cardiolipin. *Circ Res* **94**, 53-9.

Paradies, G., Petrosillo, G., Pistolese, M. and Ruggiero, F. M. (2002). Reactive oxygen species affect mitochondrial electron transport complex I activity through oxidative cardiolipin damage. *Gene* **286**, 135-41.

Pfleger, J., He, M. and Abdellatif, M. (2015). Mitochondrial complex II is a source of the reserve respiratory capacity that is regulated by metabolic sensors and promotes cell survival. *Cell Death Dis* **6**, e1835.

Potts, D. C. and Swart, P. K. (1984). Water temperature as an indicator of environmental variability on a coral reef. *Limnology and Oceanography* **29**, 504-516.

Quinlan, C. L., Orr, A. L., Perevoshchikova, I. V., Treberg, J. R., Ackrell, B. A. and Brand, M. D. (2012). Mitochondrial complex II can generate reactive oxygen species at high rates in both the forward and reverse reactions. *J Biol Chem* **287**, 27255-64.

Renshaw, G. M. and Dyson, S. E. (1999). Increased nitric oxide synthase in the vasculature of the epaulette shark brain following hypoxia. *Neuroreport* **10**, 1707-12.

Renshaw, G. M., Kerrisk, C. B. and Nilsson, G. E. (2002). The role of adenosine in the anoxic survival of the epaulette shark, Hemiscyllium ocellatum. *Comp Biochem Physiol B Biochem Mol Biol* **131**, 133-41.

Renshaw, G. M., Kutek, A. K., Grant, G. D. and Anoopkumar-Dukie, S. (2012). Forecasting elasmobranch survival following exposure to severe stressors. *Comp Biochem Physiol A Mol Integr Physiol* **162**, 101-12.

Richards, J. G., Wang, Y. S., Brauner, C. J., Gonzalez, R. J., Patrick, M. L., Schulte, P. M., Choppari-Gomes, A. R., Almeida-Val, V. M. and Val, A. L. (2007). Metabolic and ionoregulatory responses of the Amazonian cichlid, Astronotus ocellatus, to severe hypoxia. *J Comp Physiol B* **177**, 361-74.

Rolfe, D. F. and Brand, M. D. (1997). The physiological significance of mitochondrial proton leak in animal cells and tissues. *Biosci Rep* **17**, 9-16.

Rouslin, W. (1983). Mitochondrial complexes I, II, III, IV, and V in myocardial ischemia and autolysis. *Am J Physiol* **244**, H743-8.

Routley, M. H., Nilsson, G. E. and Renshaw, G. M. C. (2002). Exposure to hypoxia primes the respiratory and metabolic responses of the epaulette shark to progressive hypoxia. *Comparative Biochemistry and Physiology Part A: Molecular & Integrative Physiology* **131**, 313-321.

Rubinsky, B. (2003). Principles of Low Temperature Cell Preservation. *Heart Failure Reviews* **8**, 277-284.

Rytkonen, K. T., Renshaw, G. M., Vainio, P. P., Ashton, K. J., Williams-Pritchard, G., Leder, E. H. and Nikinmaa, M. (2012). Transcriptional responses to hypoxia are enhanced by recurrent hypoxia (hypoxic preconditioning) in the epaulette shark. *Physiol Genomics* **44**, 1090-7.

Starkov, A. (2005). Succinate in hypoxia-reperfusion induced tissue damage.

Stenslokken, K. O., Milton, S. L., Lutz, P. L., Sundin, L., Renshaw, G. M., Stecyk, J. A. and Nilsson, G. E. (2008). Effect of anoxia on the electroretinogram of three anoxia-tolerant vertebrates. *Comp Biochem Physiol A Mol Integr Physiol* **150**, 395-403.

Tretter, L., Patocs, A. and Chinopoulos, C. (2016). Succinate, an intermediate in metabolism, signal transduction, ROS, hypoxia, and tumorigenesis. *Biochim Biophys Acta* **1857**, 1086-101.

Tuan, T. C., Hsu, T. G., Fong, M. C., Hsu, C. F., Tsai, K. K., Lee, C. Y. and Kong, C. W. (2008). Deleterious effects of short-term, high-intensity exercise on immune function: evidence from leucocyte mitochondrial alterations and apoptosis. *Br J Sports Med* **42**, 11-5.

Val, A. L., Gomes, K. R. and de Almeida-Val, V. M. (2015). Rapid regulation of blood parameters under acute hypoxia in the Amazonian fish Prochilodus nigricans. *Comp Biochem Physiol A Mol Integr Physiol* **184**, 125-31.

Val, A. L. S., M. N. P.; Almeida-Val, V. M. F. (1998). Hypoxia adaptation in fish of the Amazon: a never-ending task. *South African journal of zoology. Suid-Afrikaanse tydskrif vir dierkunde.* **33**, 107-114.

Winter, J., Klumpe, I., Heger, J., Rauch, U., Schultheiss, H. P., Landmesser, U. and Dorner, A. (2016). Adenine nucleotide translocase 1 overexpression protects cardiomyocytes against hypoxia via increased ERK1/2 and AKT activation. *Cell Signal* **28**, 152-9.

Wise, G., Mulvey, J. M. and Renshaw, G. M. C. (1998). Hypoxia tolerance in the epaulette shark (Hemiscyllium ocellatum). *Journal of Experimental Zoology* **281**, 1-5.

Wojtovich, A. P. and Brookes, P. S. (2008). The endogenous mitochondrial complex II inhibitor malonate regulates mitochondrial ATP-sensitive potassium channels: implications for ischemic preconditioning. *Biochim Biophys Acta* **1777**, 882-9.

Zakharchenko, M. V., Zakharchenko, A. V., Khunderyakova, N. V., Tutukina, M. N., Simonova, M. A., Vasilieva, A. A., Romanova, O. I., Fedotcheva, N. I., Litvinova, E. G., Maevsky, E. I. et al. (2013). Burst of succinate dehydrogenase and alpha-

ketoglutarate dehydrogenase activity in concert with the expression of genes coding for respiratory chain proteins underlies short-term beneficial physiological stress in mitochondria. *Int J Biochem Cell Biol* **45**, 190-200.

Figures

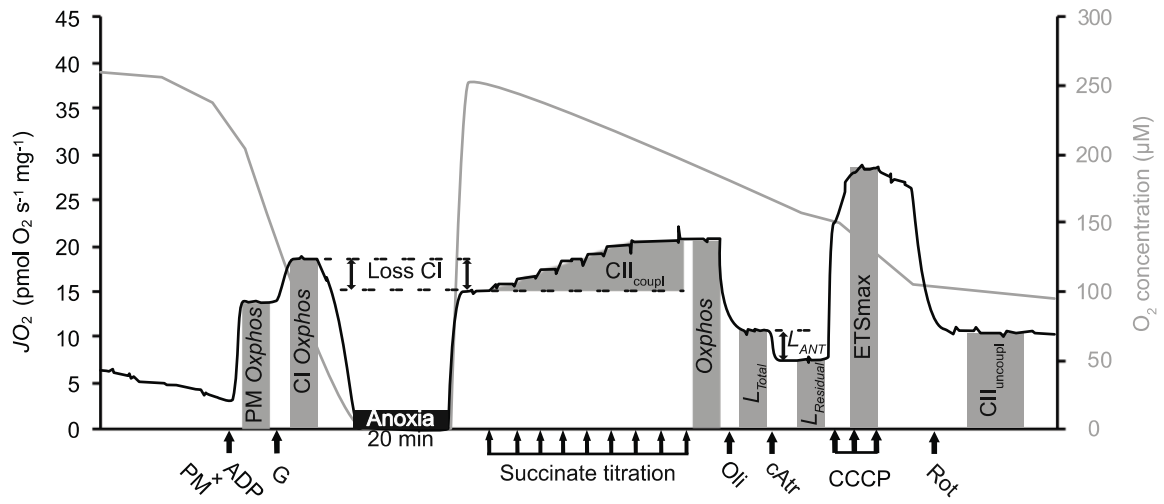

Fig. 1. Representative trace of the substrate uncoupler inhibitor protocol used to measure mitochondrial respiration rates (JO_2) of cerebellum homogenate from grey carpet sharks and epaulette sharks. Samples were introduced into the 2 ml respirometer chambers and were allowed to recover for 20 min. Excess pyruvate, malate and ADP were injected to put mitochondria into Complex I (CI) mediated oxidative phosphorylation (PM-*Oxphos*). The additive effect of glutamate was tested by inclusion in the CI substrate addition (CI-*Oxphos*). The sample was permitted to deplete O_2 until anoxia, and a reference chamber was maintained between 100-250 µM O_2 (trace not shown). The chamber was then re-oxygenated after 20 min (up to ~220 µM O_2 for both control and anoxic groups). The loss in CI mediated JO_2 (Loss CI) was calculated by anoxia exposure followed by reoxygenation (AR). Succinate was then titrated up to 10 mM to measure the contribution of CII to CI+CII-*Oxphos* ($CII_{coupled}$). At the conclusion of the experiment, oligomycin (Oli) was added to induce mitochondria in total Leak state (L_{Total}) and the contribution of the adenine nucleotide translocase (L_{ANT}) was calculated as the difference between L_{Total} and the residual leak ($L_{Residual}$), which was reached after the addition of the ANT inhibitor carboxy-atractyloside (cAtr). Finally, the mitochondria were chemically uncoupled with the titration of CCCP to determine maximum ETS capacities (ETS_{max}). Finally, rotenone was added (Rot, a CI inhibitor) to measure the uncoupled CII capacity ($CII_{uncoupled}$).

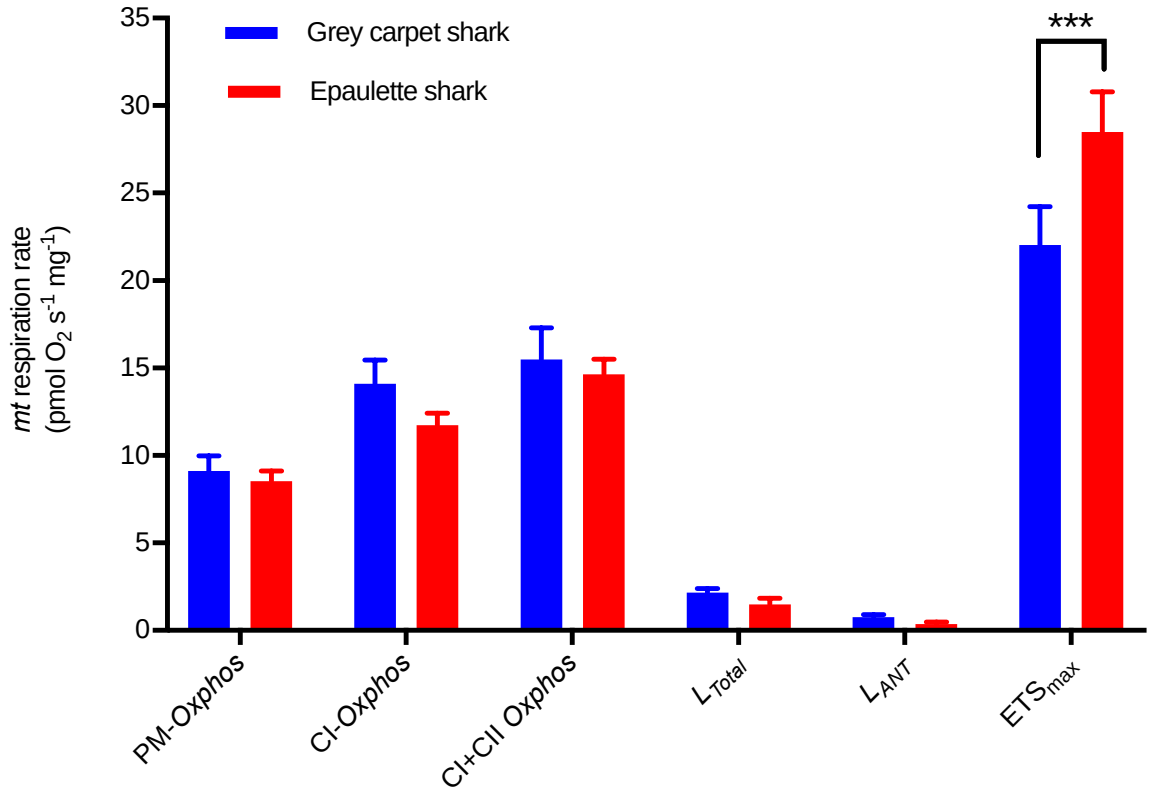

Fig. 2. Mitochondrial respiration rates in homogenates of the cerebellum from two anoxia-tolerant sharks. In PM-*Oxphos*, there was no difference in respiration rates between grey carpet sharks mitochondria (blue) and epaulette sharks mitochondria (red). The addition of excess glutamate to reach CI-*Oxphos* followed by excess succinate to reach *Oxphos* state, each mediated and increase of ~6 pmol O_2 s^{-1} mg^{-1} in both species of sharks. The addition of oligomycin to measure total leak (L_{Total}) decreased JO_2 similarly in both sharks. Adenosine nucleotide translocase mediated Leak flux (L_{ANT}), was also similar in grey carpet and epaulette sharks. However, epaulette sharks mitochondria had greater ETS capacity. Refer to the Fig. 1 legend for details on the method. Significant difference tested with two-way ANOVA and post-hoc test with Turkey correction indicated as *** at $p < 0.001$.

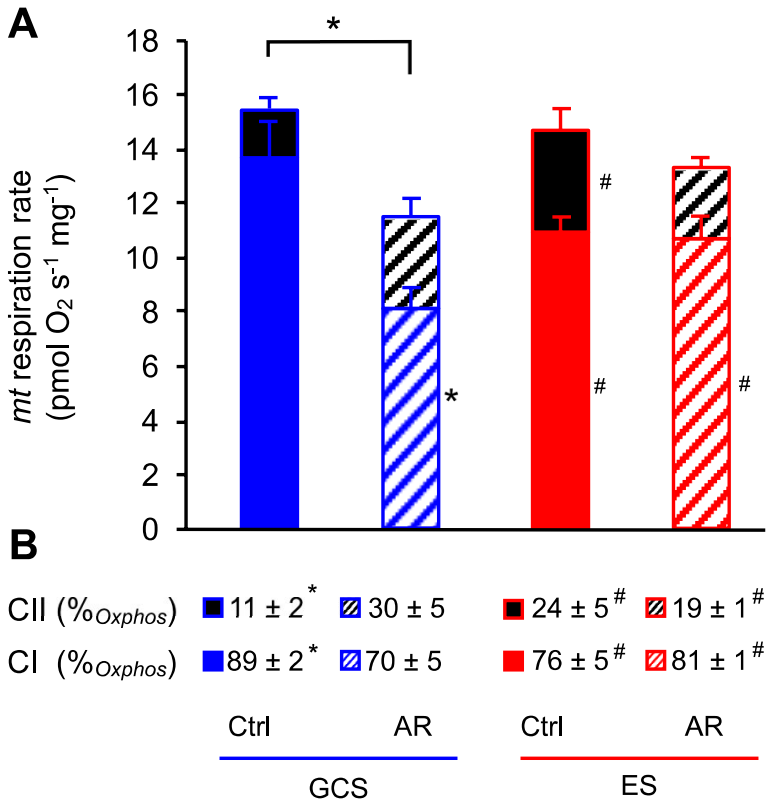

Fig. 3. Contribution of complex I and complex II to Oxphos before and after exposure to anoxia/re-oxygenation. (A) Absolute respiration rates mediated by CI (coloured) and CII (black and white) and (B) the relative contributions of each complex to Oxphos, in cerebellar homogenates of GCS (blue) and ES (red) maintained in normoxia ('Ctrl', filled) or exposed to an episode of anoxia/reoxygenation ('AR', dashed). The CI contribution to respiration was determined in the presence of excess CI-linked substrates (pyruvate, malate and glutamate) followed by ADP while the CII contribution was calculated by the additive effect of succinate on CI-mediated Oxphos respiration rates. Data in (A) represent the absolute respiration rates mediated by CI and CII, the sum of which corresponds to Oxphos rates and expressed in pmol O_2 s^{-1} mg^{-1}. Data in (B) correspond to the relative contribution of each complexes to Oxphos rates in tissue either exposed to saturated O_2 or exposed to an episode of AR. Results are expressed as mean (n = 6) ± s.e. Significant difference ($p < 0.05$) are indicated as * between treatments (Control or AR) or as # between shark species (neighbouring histograms). The additive effect of both complexes is shown as stacked histograms, tested with two-way ANOVA test with Turkey correction for multiple comparison.

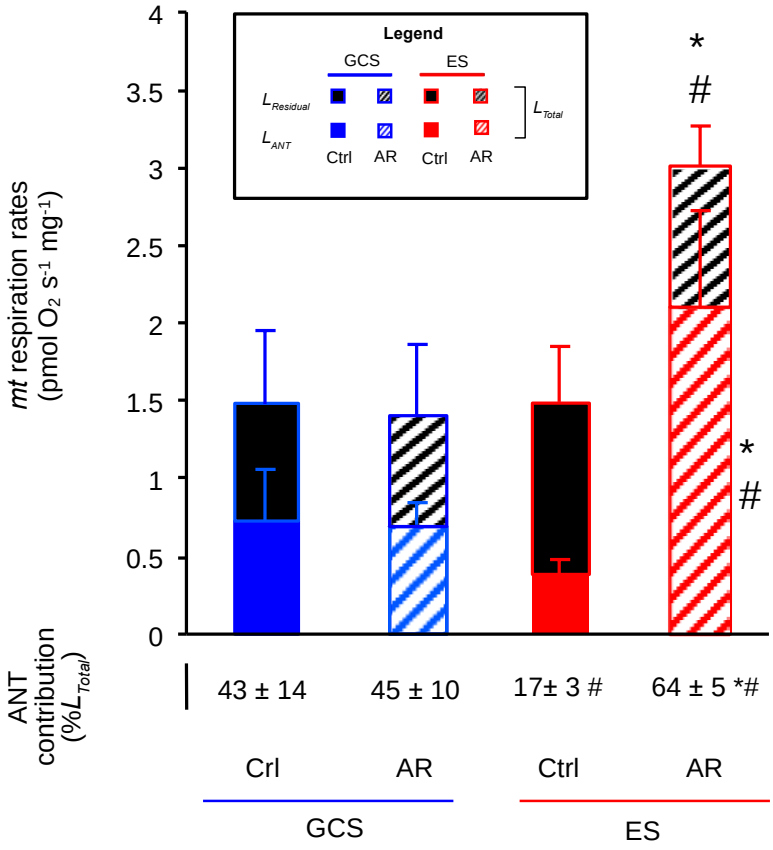

Fig. 4. Mitochondrial respiration attributed to proton leak and the contribution of the adenine nucleotide translocase (ANT). Two components of proton leak were measured in cerebellar homogenates from GCS (blue) and ES (red) that were either exposed to normoxia (Ctrl) or anoxia-reoxygenation (AR). Oligomycin was added to put phosphorylating mitochondria into the Leak state (L_{Total}). The portion of proton leak though ANT (L_{ANT}) was calculated as the difference between L_{Total} and the residual leak ($L_{Residual}$), reached after the addition of carboxy-atractyloside. Both rates are expressed as pmol O_2 s^{-1} mg^{-1} with the relative contribution of L_{ANT} to L_{Total} (values below main graph). Results presented as mean (n = 6) ± s.e. Significant difference ($p < 0.05$) indicated as * between groups (Ctrl and AR) and as # between species, tested with independent t-tests.

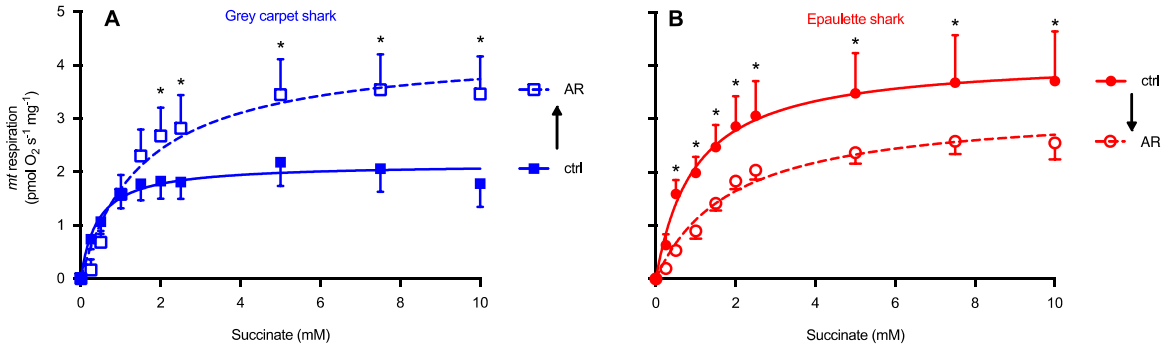

Fig. 5. Comparison of complex II respiration rates mediated by increased succinate levels. In mitochondria at normoxia ("ctrl", solid lines) or exposed to anoxia/re-oxygenation ("AR", dashed line) in cerebellum of (A) grey carpet sharks or (B) epaulette sharks. mitochondria respiration in cerebella homogenates from grey carpet sharks (blue) and epaulette sharks (red) was measured in the presence of excess CI substrates (pyruvate, malate and glutamate) and ADP. Then, succinate was titrated up to 10 mM so that CII supported JO_2 could be measured. The additive effect of succinate on JO_2 is here represented with dose-response fitted curves extracted using GraphPad Prism with the least squares method. While AR mediated an increase in CII respiration in mitochondria from grey carpet sharks, CII respiration was decreased in mitochondria of the epaulette sharks. The effect of succinate increments and AR were tested with a two-way ANOVA repeated measure test.

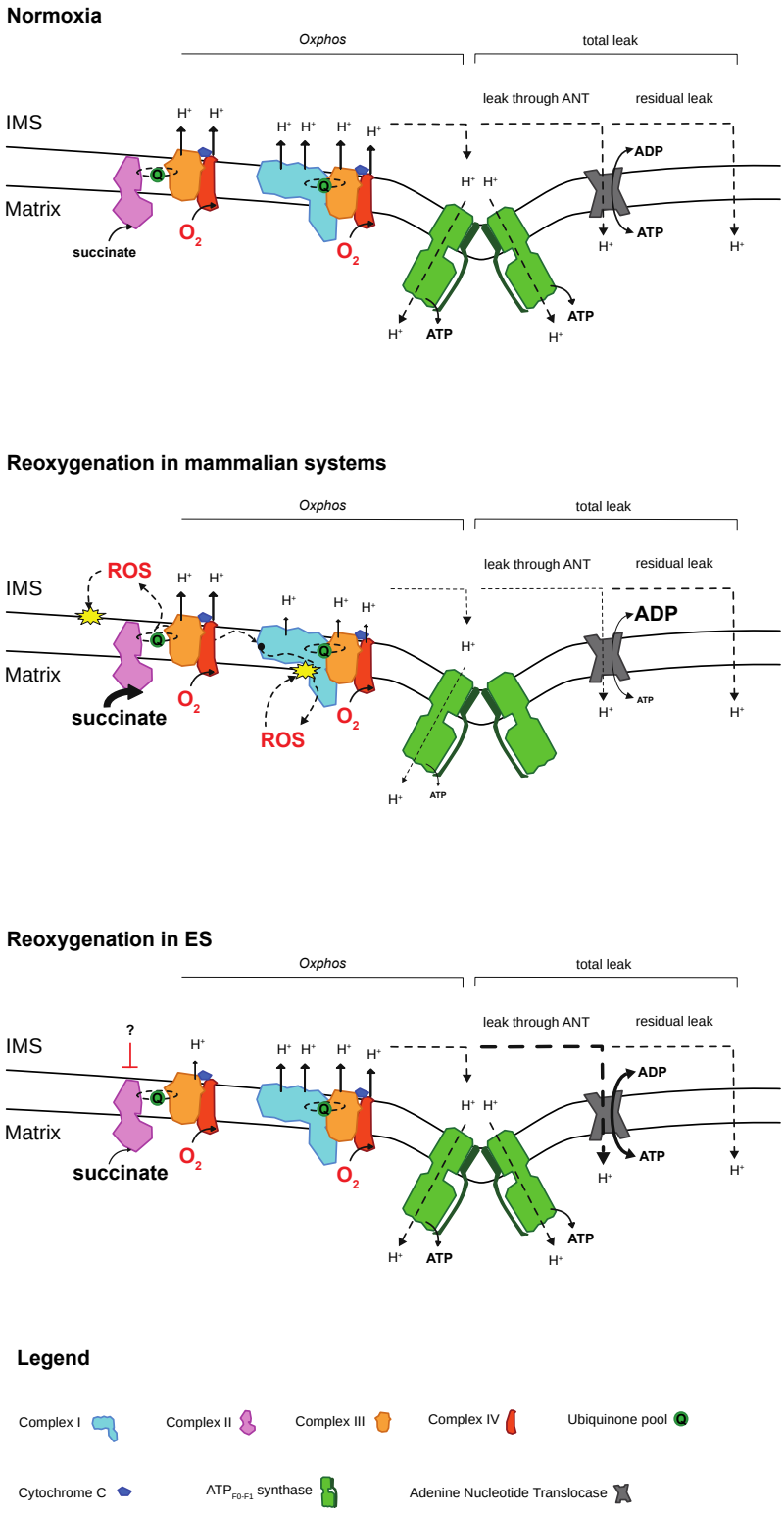

Fig. 6. Oxygen, proton and adenine nucleotide fluxes in the mitochondrial electron transport system. In normoxic conditions, proton pumping is mediated through complex I (CI) and complex II (CII) linked systems and the consumption of O_2. The gradient of proton,

more concentrated in the inter-membrane space (IMS), is utilised by the $ATP_{F0\text{-}F1}$ synthase via the process known as oxidative phosphorylation (Oxphos) to produce ATP. Some protons may leak through the membrane or transmembrane proteins, one of which being the adenine-nucleotide translocase (ANT), which mediates the ADP and ATP exchange between the matrix and the IMS. The proton leak through the ANT (L_{ANT}) and other proton leakage (residual leak) uncouple respiration from Oxphos and this results in the loss capacity to produce ATP for a given rate of respiration. After an episode of anoxia, succinate accumulates and upon re-oxygenation, succinate oxidation rate accelerates, which mediates an enhanced ROS production from CII, but also a "reverse electron flow" to CI (Chouchani et al., 2014). This likely affects CI stability and results in an overall loss of capacity for proton pumping and Oxphos. In contrast with most vertebrates, mitochondria from the epaulette shark (ES) cerebellum somehow decrease succinate oxidation rate post-AR and CI linked system capacity is maintained. The L_{ANT} was also increased post-AR and this results in the maintenance of Oxphos. The results obtained from this study suggests that the response of GCS mitochondria sits between the re-oxygenation and the ES panels. While succinate oxidation rates were increased post AR and CI-linked system capacity was decreased, the GCS maintained Oxphos rates similar to those of the ES, with a greater utilisation of O_2 for *Oxphos* (lower L_{ANT} and similar $L_{Residual}$ relative to the ES).

Table 1. Morphology of the two anoxia tolerant sharks. Body length, body mass (BM) and the ratio of the cerebellum to BM for the two anoxia tolerant shark species, grey carpet shark and the epaulette shark. The mass of the cerebellum was normalised to body mass for comparison between species. Results expressed as mean ± s.e. Significant differences between species (#) or between control and post-anoxia (*) tested with independent t-tests, $p < 0.01$).

	Body length (cm)	Body mass (g)	Cerebellum (mg) /BM (g)
Grey carpet (6)	53.00 ± 7.57	138.25 ± 30.68	8.58 ± 1.50 *
Male (2)	56.00 ± 0.01	121.91 ± 19.74	8.01 ± 0.06
Female (4)	51.00 ± 9.25	143.70 ± 31.72	8.78 ± 1.69
Epaulette (6)	67.17 ± 4.15 *	490.57 ± 82.91 *	1.19 ± 0.13
Male (3)	68.25 ± 0.25	485.57 ± 68.32	1.24 ± 0.14
Female (3)	66.63 ± 4.99	495.57 ± 95.03	1.13 ± 0.10

Table 2. Effects of anoxia/reoxygenation on mitochondrial function in cerebellum homogenates of grey carpet and epaulette sharks. The mitochondria in AR homogenates and their controls held with sufficient O_2 were uncoupled from Oxphos in the presence of rotenone to determine the CII capacity uncoupled from *Oxphos*. Three parameters of the CII capacity coupled to Oxphos were extracted using dose response curves fitted with the least-squared method and the maximum respiration rate mediated by succinate ($CII_{coupled}$) and the succinate concentration at which JO_2 is half of CII-JO_{2max} (aKm_S) were extracted using Prism7.0. The CII catalytic efficiency (CII_{cat}) was then calculated as $CII_{coupled}$ divided by aKm_S. The respiratory control ratios (RCR) is an estimation of mitochondria coupling and was calculated using the formula *Oxphos*/Leak. Net oxidative control ration was calculated as (*Oxphos*-Leak)/ETS_{max} and represents the net Oxphos capacity relative to ETS capacity. Results are expressed as mean ± s.e. Significant differences ($p < 0.05$) indicated as (*) between AR and controls or as (#) between shark species, tested with independent t-tests.

	$CII_{uncoupl}$ (pmol O_2 s^{-1} mg^{-1})	Characteristics of CII_{coupl}			ETS_{max} (pmol O_2 s^{-1} mg^{-1})	RCR	nOCR
		aKm (mM)	CII_{coupl} (pmol O_2 s^{-1} mg^{-1})	CII_{cat}			
Grey carpet shark (n = 7)							
Control	9.1 ± 0.9$^{\#}$	0.42 ± 0.18	2.0 ± 0.4$^{\#}$	4.83	22.0 ± 2.0$^{\#}$	7.9 ± 1.6	0.59 ± 0.02$^{\#}$
Anoxia/re-oxygenation	3.8 ± 0.6$^{*\#}$	1.12 ± 0.30*	3.6 ± 0.7$^{*\#}$	3.23	14.6 ± 0.9$^{*\#}$	7.4 ± 1.3*	0.66 ± 0.03$^{*\#}$
Epaulette shark (n = 7)							
Control	3.2 ± 0.5$^{\#}$	0.90 ± 0.48	4.0 ± 1.1$^{\#}$	4.47	28.5 ± 2.1$^{\#}$	9.7 ± 1.1	0.48 ± 0.04$^{\#}$
Anoxia/re-oxygenation	5.5 ± 0.6$^{*\#}$	1.37 ± 0.18	2.6 ± 0.3$^{*\#}$	1.69$^{*\#}$	19.8 ± 1.2$^{*\#}$	4.7 ± 0.7*	0.51 ± 0.03$^{\#}$